© 2004 The Chemical Society of Japan

Direct Crystallization of Amorphous Molecular Systems Prepared by Vacuum Deposition: X-ray Studies of Phenyl Halides

Hideyuki Nakayama,* Shin-ichi Ohta, Iji Onozuka, Yuichi Nakahara, and Kikujiro Ishii

Department of Chemistry, Gakushuin University, 1-5-1 Mejiro, Toshimaku, Tokyo 171-8588

Received November 10, 2003; E-mail: hideyuki.nakayama@gakushuin.ac.jp

Many amorphous molecular systems prepared by vacuum deposition onto cold substrates turn into crystals directly without exhibiting glass transition when their temperature is raised. To study the mechanism of the crystallization from amorphous states, we monitored the increase of X-ray Bragg peaks at constant temperatures for fluoro-, chloro-, and bromobenzene samples. Data were analyzed by using the Johnson–Mehl–Avrami equation. It was found that the crystallization from amorphous states of these compounds progresses through the nucleation and crystal-growth processes similar to those observed for fused materials. However, slightly complicated behaviors were observed for molecules with larger substituents. These are considered to arise from the wide distribution of molecular arrangements that are stochastically generated in samples by the vapor deposition at low temperatures.

Amorphous states are non-equilibrium states, and the materials tend to change the structures toward more stable states. This tendency is sometimes revealed by structural relaxation or crystallization. As for amorphous systems with molecular nature, many studies have been made in relation to the glass transition.[1,2] In these studies, characteristic relaxation phenomena and non-Arrhenius behavior of viscosity in the supercooled-liquid state have attracted attention of workers, but the mechanism of the glass transition has not yet been elucidated enough. On the other hand, few studies have been made on the structural relaxation or crystallization in amorphous molecular systems that do not undergo the glass transition.[3,4]

Unlike the crystallization from fused states, the concept of the direct crystallization from amorphous states, that is the subject of the present study, might not be acceptable, because the atoms or molecules are considered to be frozen in solid states. It had been generally considered until the early 1970s that the crystallization might not occur below the glass-transition temperature.[5,6] However, direct crystallizations from amorphous states have been observed for metaphosphate glasses[7] and metallic glasses.[8] In addition, direct crystallizations in amorphous molecular systems have been confirmed in the 1990s. Takeda et al.[9] studied the thermal properties of vapor-deposited *n*-alkanes and their binary systems by differential thermal analysis, and showed that the crystallization in amorphous butane takes place below the expected glass-transition temperature. We have systematically studied the relaxation processes of the vapor-deposited amorphous samples of simple organic compounds by vibrational spectroscopies and X-ray diffraction.[4,10–14] It has been found that there are two types of processes when the temperature of amorphous samples is raised. One is the direct crystallization from amorphous states and the other is the glass transition followed by crystallization. Amorphous samples of chlorobenzene and bromobenzene show the direct crystallization, the crystallization temperatures being lower than their expected glass-transition temperatures by about 20 and 30 K, respectively.[10,15] Furthermore, amorphous samples of aromatic compounds such as anthracene[12] and biphenyl,[13] and of long-chain hydrocarbons such as $C_{24}H_{50}$,[14] also crystallize from the amorphous state, but the crystallization processes are complicated. Okamoto et al.[16] reported an example where the nucleation below the glass-transition temperature occurs in the amorphous state of a compound that exhibits the glass transition. However, the study of the direct crystallization in amorphous molecular states has only arrived at the starting line.

Recently, we have studied the relaxation processes of chlorobenzene/toluene[17] and chlorobenzene/ethylbenzene[18] binary systems as the function of composition. It was found that the characteristic temperatures of the direct crystallization, glass transition, and crystallization from the supercooled liquid came across each other in a certain region of concentration. There is a possibility that the mechanism of the direct crystallization has some relation to those of the glass transition and the crystallization from the supercooled liquid. Therefore, it is important to elucidate the mechanism of direct crystallization from amorphous states. In this paper, we report the results of X-ray studies on the crystallization process of amorphous molecular systems. We chose fluoro-, chloro-, and bromobenzenes as the object compounds, since they crystallize from amorphous states with good reproducibility without exhibiting the glass transition.[10] Hereafter, fluoro-, chloro-, and bromobenzenes are abbreviated to FB, CB, and BB, respectively. We apply to the data analysis the well-known Johnson–Mehr–Avrami (JMA) equation[19,20] which is usually used for the analysis of the crystallizations in fused materials, and discuss the mechanism of the direct crystallizations in amorphous states.

Experimental

Commercial FB (Koso Chemical), CB (Wako Pure Chemical Industries), and BB (Tokyo Kasei Kogyo) were used after distillation and fractional crystallization. Amorphous samples were prepared by the vapor deposition onto the cold substrate in the previously reported vacuum chamber[4] with the base pressure below 10^{-5} Pa. The substrate was a gold-plated copper block with the

Published on the web June 9, 2004; DOI 10.1246/bcsj.77.1117

area of $30 \times 30\ mm^2$. The thickness of the samples was made to be about 10 μm by monitoring the interference of transmitted laser light.[21] After the deposition, the temperature of the sample was raised rapidly up to the annealing temperature, and the increase of the intensity of X-diffraction peaks was measured by keeping the temperature constant at that temperature.

X-ray diffraction was measured using the system reported previously.[4] A Cu X-ray source was used at 40 kV and 20 mA, and was fixed in most of the measurements at the incident angle of 2 degrees. The diffraction patterns were recorded by scanning the detector arm on which a graphite monochromator was equipped for removing the K_β X-ray lines.

Results

In Table 1, we summarize the deposition temperatures and the annealing-temperature regions in which the crystallization process was monitored for the three compounds. In the same table, the observed activation energies of the direct crystallization and enthalpy of vaporization are also indicated. The annealing temperature region for each compound was taken around the temperature at which the direct crystallization was observed within the experimental time scale.[10] Two different deposition temperatures were examined for each compound, since the degree of disorder has been known to be different for samples deposited at different temperatures.[21] Thus the deposition temperatures were set to be about 0.25 and 0.75 times the annealing temperature. After the sample deposition, the sample temperature was raised rapidly to each annealing temperature with a rate of about 5 K/min; then, X-ray measurements were carried out by keeping the temperature constant at the annealing temperature.

Figure 1 shows the X-ray diffraction patterns of the three compounds: (a) immediately after the deposition at temperatures indicated, and (b) after the crystallization at temperatures indicated. No sharp Bragg peak was observed in the diffraction patterns of all the samples immediately after the deposition; only a broad diffraction hump was observed, indicating that they were in amorphous sates. On the other hand, the diffraction patterns observed after the crystallization showed the characteristics of the crystal of each compound regardless of the differences in the deposition and annealing temperatures. Namely, the amorphous state of each compound relaxes into the crystal state that has the same structure regardless of the preparation and annealing conditions. In the crystallization process from amorphous states, metastable crystalline phases sometimes appear before reaching the stable crystalline phase.[22] Therefore, the crystalline states obtained in the present study are not necessarily stable states. We compared the obtained results with the literature data,[23–25] although the temperature (and pressure in the case of CB) were somewhat different from the present conditions, and only the space symmetry and cell parameters have been reported for BB. The observed diffraction pattern of each compound was almost reproduced using the literature data, Miller indices of principal peaks being indicated in Fig. 1. It was confirmed that anisotropic distribution of the orientation of the micro-crystals in the sample was small by comparing the diffraction patterns obtained with different modes of the scanning of the detector and X-ray source arms.

Table 1. Deposition Temperatures, Annealing Temperature Regions in Which Direct Crystallization Was Observed, Activation Energies of Crystallization, and Enthalpy of Vaporization for Three Compounds

	Deposition temperature /K	Annealing temperature region/K	Activation energy /kJ mol^{-1}	Enthalpy of vaporization[a] /kJ mol^{-1}
FB	20	82–85	29	34.6
	65	82–86	34	
CB	25	103–107	(42)	41.0
	78	101–105	36	
BB	25	106–110	30	44.5
	80	102–109	35	

a) Ref. 31.

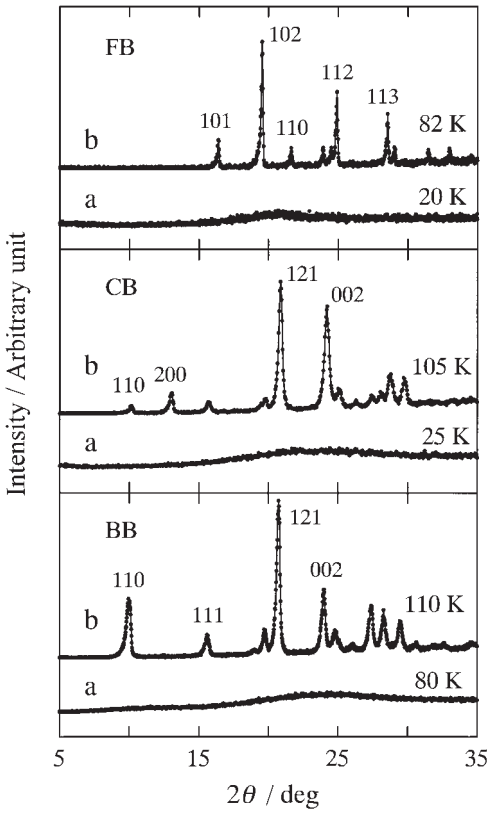

Fig. 1. X-ray diffraction patterns of the three compounds and assignment of principal peaks. (a) Immediately after the deposition at the temperatures indicated. (b) After the crystallization at the temperatures indicated.

Figure 2 shows an example of the evolution of diffraction peaks during the annealing at a constant temperature. It took 3 min to record each pattern. The sample was FB deposited at 20 K and annealed at 83.5 K. No Bragg peak was seen in the diffraction pattern immediately after the temperature was raised to 83.5 K, but after about 3 h peaks appeared and these increased their intensity gradually. Similar evolutions were observed for other samples, but for CB deposited at 25 K, Bragg peaks were observed at the initial stage when the temperature was set at the annealing temperature. This may be related to the large degree of disorder in the sample deposited at a very low temperature, and will be discussed later.

The changes in the integral intensity of the most prominent

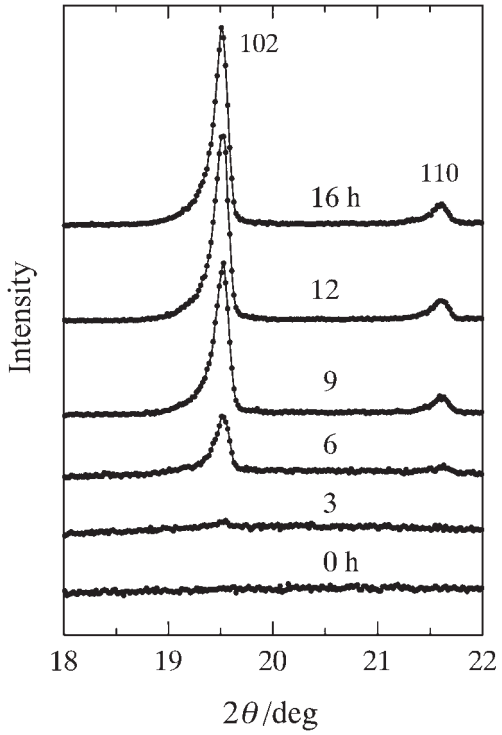

Fig. 2. Evolution of the 102 and 110 diffraction peaks of FB deposited at 20 K due to the annealing at 83.5 K.

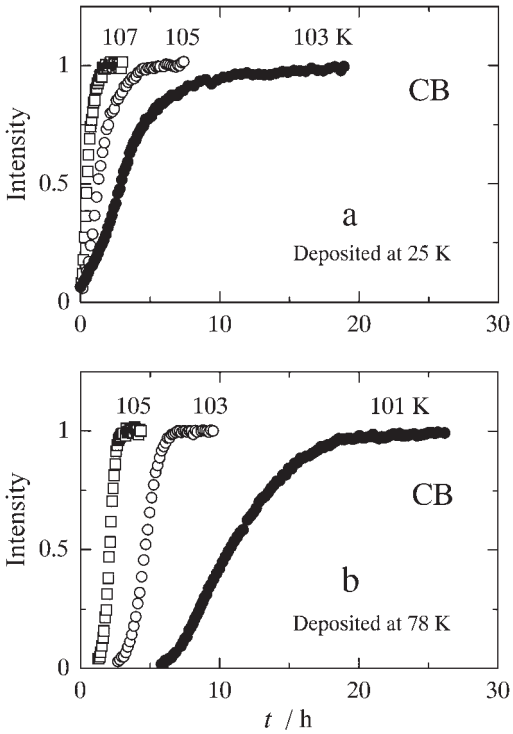

Fig. 4. Increase of the integral intensity of the 121 X-ray peak of CB during the annealing at a constant temperature indicated; (a) Samples deposited at 25 K, (b) Samples deposited at 78 K. The ordinate is the value normalized by the saturating value after a long annealing.

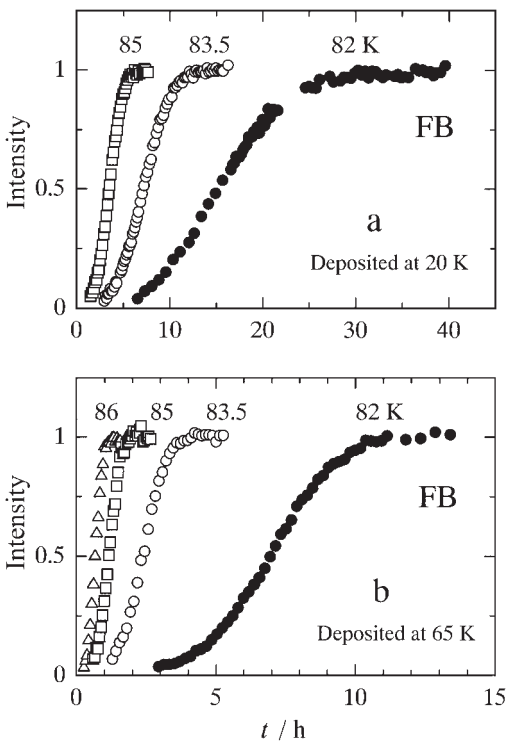

Fig. 3. Increase of the integral intensity of the 102 X-ray peak of FB during the annealing at a constant temperature indicated; (a) Samples deposited at 20 K, (b) Samples deposited at 65 K. The ordinate is the value normalized by the saturating value after a long annealing.

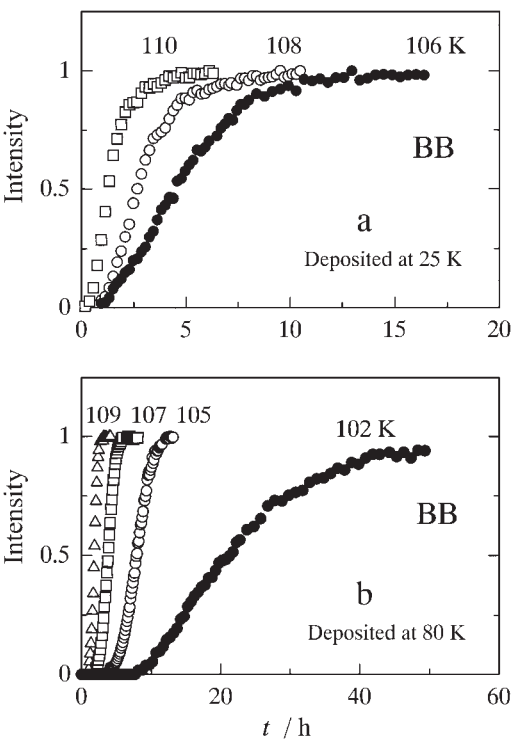

Fig. 5. Increase of the integral intensity of the 121 X-ray peak of BB during the annealing at a constant temperature indicated; (a) Samples deposited at 25 K, (b) Samples deposited at 80 K. The ordinate is the value normalized by the saturating value after a long annealing.

Bragg peak of FB, CB, and BB are shown in Figs. 3–5, respectively, for different annealing temperatures. For CB, we reproduce here the data in our previous paper[21] to compare with those of other compounds. The intensity is normalized by the saturation value at each annealing temperature. Thus the ordinate indicates the fraction of the crystalline part to the total amount that finally crystallized at each annealing temperature. Further increases in intensity by 3–10% were observed for many samples when the temperature was raised further by about 50 K after the intensity was saturated at an annealing temperature. Therefore, a part of more than 90% of each sample finally crystallized at each annealing temperature. We considered that the remaining part of the sample had structures very unfavorable for the crystal growth at the annealing temperature and then we excluded such parts from the analysis. The results shown in Figs. 3–5 indicate: (1) the crystallization rate of the samples with the same deposition temperature is faster if the annealing temperature is higher; (2) the crystallization rate of the samples with the same annealing temperature is faster if the deposition temperature is higher. For example, the FB samples deposited at 20 K and 65 K needed 15 and 7 h, respectively, for the annealing at 82 K until the normalized intensity reached 0.5.

Discussion

JMA Plot of the Data for Each Sample. The crystallization kinetics were analyzed by means of the Johnson–Mehl–Avrami (JMA) equation[19,20]

$$x = 1 - \exp(-kt^n) \tag{1}$$

where x is the crystalline fraction at time t, n is a parameter related to the crystallization mechanism, and k is a parameter related to the nucleation rate, crystal-growth rate, and crystallization mechanism. This equation has been used to analyze the kinetics of the crystallization under isothermal conditions. This has been used not only for the crystallization from fused sates,[26] but also for the direct crystallization of metallic glasses[27] and of amorphous ice.[28] However, the present study is the first one in which the JMA equation is used for the analysis of direct crystallization of amorphous molecular systems prepared by vapor deposition.

Equation 1 can be transformed into the following form:

$$\ln[-\ln(1-x)] = \ln k + n \ln t. \tag{2}$$

Thus, the plot of $\ln[-\ln(1-x)]$ against $\ln t$ (the JMA plot) may be linear if k and n are constant. Then the value of n is obtained from the slope of the straight line. JMA plots of the data for all the samples in Figs. 3–5 are shown in Figs. 6–8. Solid lines shown in the figures are the results of the linear fitting for selected regions of the data.

For FB, JMA plots of all the data obtained at different conditions are well fitted with straight lines. This indicates that the direct crystallization of amorphous FB took place by a single process involving the nucleation and crystal growth throughout the whole crystallization process. For the samples deposited at 20 K, the value of n are in the range of 3.0–3.4. For the samples

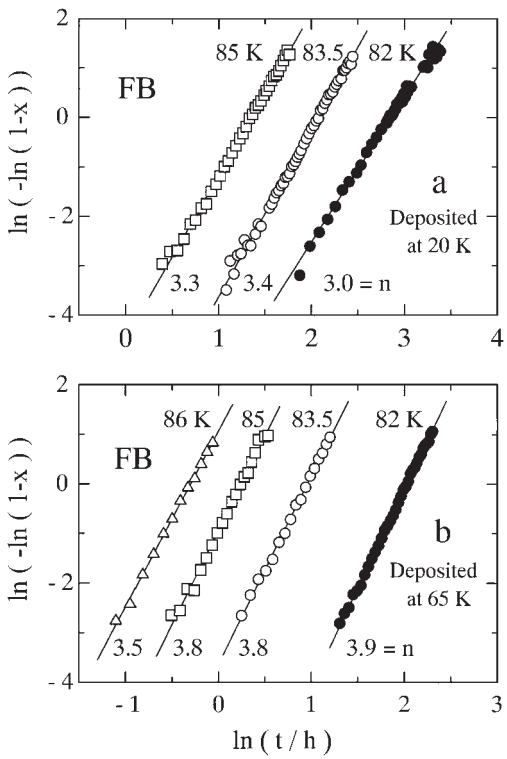

Fig. 6. JMA plots of X-ray data for FB in Fig. 3. Solids lines represent the linear fitting and the n value indicates the slope of each line; (a) Samples deposited at 20 K, (b) Samples deposited at 65 K.

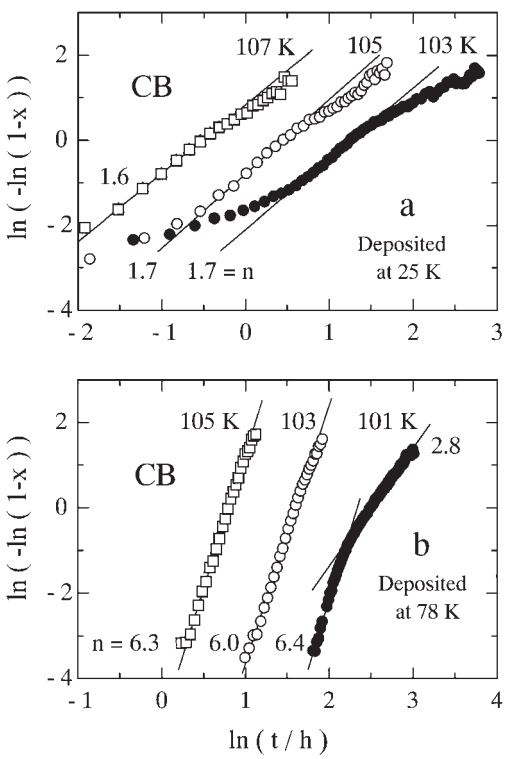

Fig. 7. JMA plots of X-ray data for CB in Fig. 4. Solids lines represent the linear fitting and the n value indicates the slope of each line; (a) Samples deposited at 25 K, (b) Samples deposited at 78 K.

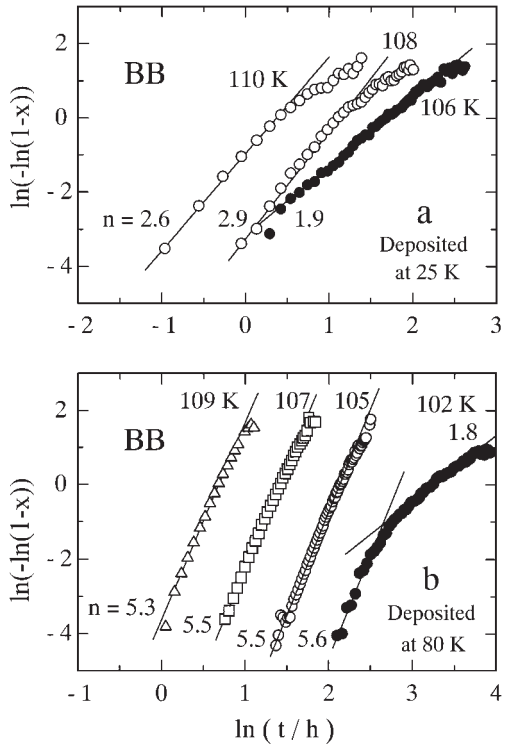

Fig. 8. JMA plots of X-ray data for BB in Fig. 5. Solids lines represent the linear fitting and the n value indicates the slope of each line; (a) Samples deposited at 25 K, (b) Samples deposited at 80 K.

deposited at 65 K, n falls in the range of 3.5–3.9. The relation between the n value and the crystallization mechanism has been studied well.[29] $n = 3$ corresponds to the three-dimensional crystal growth under the conditions of constant nucleus number and constant growth rate, or corresponds to the two-dimensional crystal growth under the conditions of constant nucleation rate and constant growth rate. $n = 4$ corresponds to the three-dimensional crystal growth under the conditions of constant nucleation rate and constant crystal-growth rate. We consider that the difference in n is related to the nucleation condition, since the dimensionality of the crystal growth, or the habit of the resultant crystals in other words, may be similar for the crystals of the same compound appearing at almost the same annealing temperature. Thus the obtained values of n between 3 and 4 suggest that the samples deposited at 20 K crystallized with small contributions of new nuclei, and that the samples deposited at 65 K crystallized with increasing contribution of freshly generated nuclei.

JMA plots of CB depend on both the deposition and annealing temperatures (Fig. 7). For the samples deposited at 25 K, deviation from straight lines is obvious. However, we tried to estimate n values from the middle part of the plots. The results are about 1.7. These values suggest that the crystallization was assisted by nuclei existing in the sample in advance, and that the crystals grew with constant numbers of nuclei. It has been mentioned above that Bragg peaks were observed at the stage when the CB samples deposited at 25 K reached the annealing temperature. Namely, the crystallization took place without an induction period. This issue will be discussed later again in relation to the density inhomogeneity in amorphous samples deposited at low temperatures.

For the CB samples deposited at 78 K, JMA plots for the samples annealed at 105 and 103 K are almost linear with the n values of 6.3 and 6.0, respectively. From these values, crystallization processes with the increase of nucleation rate are suggested.[29] On the other hand, the plot for the sample annealed at 101 K changes its slope around $x = 0.4$. Thus n changed from 6.4 to 2.8. Although the mechanism cannot be identified uniquely from these values, it is considered that the nucleation rate increased in the early stage of the crystallization, but it decreased later.

JMA plots for BB show features similar to those for CB, depending on both the deposition and annealing temperatures. Almost linear plots were obtained for the samples deposited at 80 K except for the sample annealed at 102 K. The n values were in the range of 5.3–5.5. These values are attributed to the crystallization with increasing nucleation rates. The plot for the sample annealed at 102 K after the deposition at 80 K has almost the same n value as the above samples at the early stage of crystallization, but the plot curves later remarkably to the n value of about 1.8. This behavior is similar to that of the CB sample deposited at 78 K and annealed at 101 K, indicating a change in the nucleation rate. For the samples annealed at 110 K or 108 K after the deposition at 25 K, linear plots were obtained until about $x = 0.7$, and n was 2.6 and 2.9, respectively. Although the mechanism cannot be identified from these values, the results are very similar to those obtained for CB, that is, n values are smaller for samples deposited at lower temperatures than for samples deposited at higher temperatures. For the sample annealed at 106 K after the deposition at 25 K, a linear plot was obtained in the region $x = 0.1$–0.8, and $n = 1.9$ was obtained. This indicates the crystal growth with a constant number of nuclei.

General Features of the JMA Plots. We have described so far the crystallization behavior of amorphous phenyl halides on the basis of the JMA plots. We have noticed as the general feature that the data for FB samples are adoptable well to the JMA plot, while the plots for CB and BB samples show (a) the large dependence of n on the deposition and annealing temperatures, and (b) the bending for some samples.

The results for FB suggest that the crystallization involves the nucleation and growth processes. This is similar to the crystallization in fused materials, but the manner of the molecular diffusion in the amorphous state might be different from that in fused materials (see the later discussion). The slight difference between the n values for FB samples deposited at 20 and 65 K may be attributable to the nucleation condition. Namely, there is a tendency that the number of nuclei increases during the annealing of the samples deposited at 65 K, but this increase is not considerable for the samples deposited at 20 K.

For CB and BB samples, several complicated features of the crystallization have been revealed. For the samples deposited at high temperatures, the JMA plot seems to be adoptable to some extent, but a convex bending of the plot occurs if the annealing temperature is not high enough. See the data for the 101 K annealing of the CB sample deposited at 78 K (Fig. 7) and the data for the 102 K annealing of the BB sample deposited at 80 K (Fig. 8). The bending seen for the above samples suggest that

the increase of the nucleation rate was stopped when the crystallization have progressed to a certain fraction of the whole sample. The fact that such bending was seen for CB and BB samples but not for FB samples implies that the barrier for the molecular diffusion in amorphous solids is more firm in CB and BB samples than in FB samples.

The second remarkable feature in the JMA plots for CB and BB samples is that the n values are much smaller for the samples deposited at 25 K than those for the samples deposited at 78 or 80 K. The large n values for the samples deposited at high temperatures imply that the number of nuclei is initially small but increases acceleratedly as the crystallization progresses. On the other hand, the small n values for the samples deposited at 25 K imply that the crystallization took place with almost constant numbers of nuclei.

In the JMA plots for CB and BB samples deposited at 25 K, one may also notice that the plots show slightly convex bending in the final stage of the crystallization. This indicates serious slowdown of the crystallization in almost crystallized samples, and may reflect the existence of a small fraction of the sample where the molecular arrangements are not favorable for the crystallization. This is in good contrast with the fact that the plots for the CB samples deposited at 25 K show slightly concave bending in the initial stage of the crystallization. The latter phenomenon is considered to reflect the existence in the initial samples of the molecular arrangements very favorable for the crystallization. Such molecular arrangements may be stochastically generated in the sample in the vapor-deposition process onto the substrate at very-low temperatures, and may have locally high density and high enthalpy. Thus some relaxation around the site containing such molecular arrangements releases the excess enthalpy and causes the nucleation at temperatures much lower than the temperature where the nucleation takes place in the normal amorphous state of the compound.

Crystallization Mechanism and Density Inhomogeneity in Vapor-Deposited Amorphous Samples. In the vapor-deposition processes, the kinetic energy of the deposited molecules is taken away rapidly by the cold substrate, and the molecules are prevented from taking stable packing. Thus the amorphous samples obtained by this method may have structural features that depend on the deposition temperature. One is related to the density inhomogeneity. We have reported previously that amorphous CB samples deposited at very-low temperatures incorporate serious density inhomogeneity.[21] The existence of inhomogeneity was found by the observation of the intensity decrement of transmission light during the sample deposition below 40 K, while the sample deposited at 78 K kept good transparency even for the deposition thickness up to about 10 μm. Similar intensity decrements were observed for the FB and BB samples deposited at 20 and 25 K, respectively. Therefore, these samples are also considered to have incorporated density inhomogeneity to a degree similar to that of CB samples deposited below 40 K.

As another structural feature dependent on the deposition temperature, it has been known that vapor-deposited amorphous samples have a higher enthalpy if the deposition temperature is lower.[3] This means that molecular packing is less stable as the deposition temperature is lower. In addition, we recently found that the densities of vapor-deposited samples are lower than the fictitious values expected for the supercooled liquids at the same temperatures.[30] From all above results, amorphous samples deposited at very-low temperatures are considered to incorporate unstable and inhomogeneous molecular packing and to have low densities.

Orientational and positional rearrangements of molecules are necessary for amorphous molecular systems to crystallize. The energy barriers against these rearrangements depend on the molecular packing in the sample. If the deposition temperature is low, the resultant molecular packing may be inhomogeneous, involving a wide distribution of barrier heights. When such a sample is annealed at a constant temperature where thermal movement of molecules is restricted, molecules with low-energy barriers may contribute to the early stage of the crystallization, but the supply of molecules for growing crystals may decrease as the crystallization progresses. This explains the small induction time and small n value for the crystallization of the samples deposited at very-low temperatures. On the other hand, in a sample with narrow distribution of the barrier heights, molecular motions related to the nucleation and crystal growth are inhibited if the annealing temperature is not high enough. However, once molecular rearrangements at a nucleus start, new movements of nucleation at neighboring sites are induced. This means first that some induction time may accompany the crystallization of such samples, and second, that the number of nuclei acceleratedly increases during the crystallization process, giving a large n value.

The above inferences match the observed characteristics of the time evolution of X-ray diffraction of CB and BB samples, and explain the large difference between the behaviors of the samples deposited at low and high temperatures. In the case of FB, however, the n value did not show a large dependence on the deposition temperature, although similar difference in the transparency was observed between the samples deposited at low and high temperatures. The small size of the fluorine atom is considered to explain these results.

Apparent Activation Energy of the Crystal Growth. As has been shown in Figs. 3–5, we measured the time evolution of the X-ray diffraction intensity for the vapor-deposited samples by changing the annealing temperature. We estimated the apparent activation energy of crystal growth by the Arrhenius plot of the time $\tau_{1/2}$ where the diffraction intensity reached half the saturated intensity. The results for FB are shown in Fig. 9. We similarly plotted $\tau_{1/2}$ for CB and BB samples, and the activation energies obtained from the slopes of the plots are summarized in Table 1. The value for CB deposited at 25 K is indicated in parentheses. This means that the value is not reliable because the growth of the Bragg peaks was already observed weakly when the temperature of the samples was elevated to the annealing temperatures. However, it is noteworthy that all the apparent activation energies for the crystal growth in present samples fall in the region of 30–40 kJ mol^{-1}, although the temperature intervals used for the slope estimation were very narrow.

It is roughly considered that the energy required to generate a void in a liquid is of the order of the energy needed to evaporate the molecules occupying the same volume.[32] For the three compounds studied, the enthalpy of vaporization at room temperature are summarized in Table 1. Apparently, the activation en-

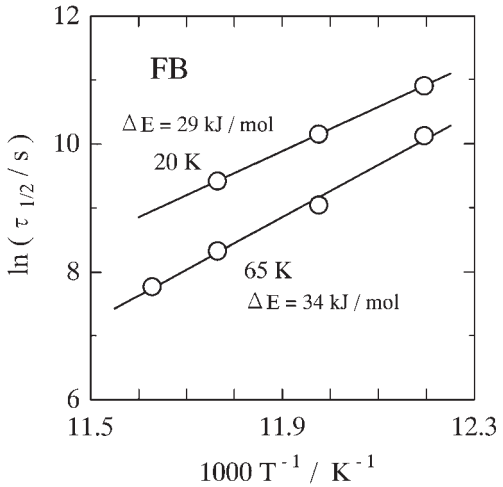

Fig. 9. Arrhenius plots of $\tau_{1/2}$ for FB. $\tau_{1/2}$ indicates the time when the diffraction intensity reached half saturation intensity. The slopes give the apparent activation energy of the crystal growth.

ergies are comparable to the corresponding enthalpies of vaporization, and might be smaller for the samples deposited at lower temperature. We consider that the latter point is related to the density inhomogeneity in the samples deposited at low temperatures. Although the number of samples and the number of the examined conditions of the deposition and annealing were small, the above results imply that thermal generation of void is needed for the crystal growth in amorphous molecular solids. Molecular motions in such voids may be distinguished from those in fused phases. It should be emphasized that the molecular motions in the narrow space in the solid may play important roles in the direct crystallization of amorphous molecular systems.

Finally we compare the molecular motion related to the direct crystallization with the relaxational motion in supercooled liquids. It has been considered for molecular liquids that there are two types of relaxations called α and β relaxations.[33] The former might be attributed to molecular motions in clusters that appear near the glass-transition temperature T_g. The latter might be attributed to molecular motions outside the clusters. The relaxation time of the α process is elongated as the temperature is lowered toward T_g. Since the direct crystallization phenomena studied in the present work are considered to occur at temperatures much lower than the expected T_g of each compound,[10] the molecular motions related to the α process must be frozen. Thus, if we seek the relationship with liquids, the β relaxation has a possibility to be connected with the molecular motions responsible for the direct crystallization. Further studies are needed for more detailed discussions.

Conclusion

Direct crystallization phenomena were studied with X-ray diffraction for the vapor-deposited amorphous samples of three kinds of phenyl halides. It was confirmed that the direct crystallization from the amorphous state takes place in a narrow-temperature region characteristic of each compound if the condition of the sample preparation is kept constant. For most of the samples, the JMA plot is adoptable to the analysis of the crystallization process, which indicates that the process involving the nucleation and crystal growth takes place in many amorphous molecular systems as in fused materials. It was pointed out, however, that the manner of the molecular diffusion related to the crystal growth may be somewhat different from that in fused materials. For the samples of the compounds with large substituents on the phenyl ring, complicated evolutions of the diffraction intensity are sometimes observed. These are attributed to the wide distribution of molecular arrangements in the initial sample prepared by the vapor deposition on the substrate at very-low temperatures.

References

1 C. A. Angell, K. L. Ngai, G. B. McKenna, P. F. McMillan, and S. W. Martin, *J. Appl. Phys.*, **88**, 3113 (2000).
2 P. G. Debenedetti and F. H. Stillinger, *Nature*, **410**, 259 (2001).
3 M. Oguni, H. Hikawa, and H. Suga, *Thermochim. Acta*, **158**, 143 (1990).
4 K. Ishii, H. Nakayama, T. Yoshida, H. Usui, and K. Koyama, *Bull. Chem. Soc. Jpn.*, **69**, 2831 (1996).
5 T. P. Seward, "Phase Diagrams," ed by A. M. Alper, Academic Press, New York (1970), Vol. 1, pp. 295–338.
6 M. Sugisaki, H. Suga, and S. Seki, *Bull. Chem. Soc. Jpn.*, **41**, 2586 (1968).
7 Y. Abe, *Nature*, **282**, 55 (1979).
8 F. E. Luborsky, *Mater. Sci. Eng.*, **28**, 139 (1977).
9 K. Takeda, M. Oguni, and H. Suga, *J. Phys. Chem. Solids*, **52**, 991 (1991).
10 H. Nakayama, H. Usui, and K. Ishii, *Prog. Theor. Phys. Suppl.*, **126**, 115 (1997).
11 K. Ishii, H. Nakayama, K. Koyama, Y. Yokoyama, and Y. Ohashi, *Bull. Chem. Soc. Jpn.*, **70**, 2085 (1997).
12 K. Ishii, H. Nakayama, Y. Yagasaki, K. Ando, and M. Kawahara, *Chem. Phys. Lett.*, **222**, 117 (1994).
13 K. Ishii, H. Nakayama, K. Tanabe, and M. Kawahara, *Chem. Phys. Lett.*, **198**, 236 (1992).
14 K. Ishii, M. Nukaga, Y. Hibino, S. Hagiwara, and H. Nakayama, *Bull. Chem. Soc. Jpn.*, **68**, 1323 (1995).
15 C. A. Angell, J. M. Sare, and E. J. Sare, *J. Phys. Chem.*, **82**, 2622 (1978).
16 N. Okamoto, M. Oguni, and Y. Sagawa, *J. Phys.: Condens. Matter*, **9**, 9187 (1997).
17 M. Murai, H. Nakayama, and K. Ishii, *J. Therm. Anal. Calorim.*, **69**, 953 (2002).
18 K. Ishii, M. Murai, M. Yamamoto, M. Takei, and H. Nakayama, to be published.
19 W. A. Johnson and K. F. Mehl, *Trans. AIME*, **135**, 315 (1981).
20 M. Avrami, *J. Chem. Phys.*, **9**, 177 (1941).
21 K. Ishii, M. Yoshida, K. Suzuki, H. Sakurai, T. Shimayama, and H. Nakayama, *Bull. Chem. Soc. Jpn.*, **74**, 435 (2001).
22 H. Nakayama, M. Kawahara, and K. Ishii, *Chem. Phys.*, **178**, 371 (1993).
23 V. R. Thalladi, H.-C. Weiss, D. Blaser, R. Boese, A. Nangia, and G. R. Desiraju, *J. Am. Chem. Soc.*, **120**, 8702 (1998).
24 P. D. Andre, R. Fourme, and M. Renaud, *Acta Crystallogr.*, **B27**, 2371 (1971).
25 D. E. Henshaw, *Acta Crystallogr.*, **14**, 1080 (1961).
26 D.-S. G. Hu and H.-J. Liu, *Macromol. Chem. Phys.*, **195**,

1213 (1994).
27 M. G. Scott, *J. Mater. Sci.*, **13**, 291 (1978).
28 W. Hage, A. Hallbrucker, E. Mayer, and G. P. Johari, *J. Chem. Phys.*, **103**, 545 (1995).
29 J. W. Christian, "The Theory of Transformation in Metals and Alloys," 2nd ed, Pergamon Press, Oxford (1975), Part 1, pp. 15–20, pp. 525–542.
30 K. Ishii, H. Nakayama, T. Okamura, M. Yamamoto, and T. Hosokawa, *J. Phys. Chem.*, **107**, 876 (2003).
31 "CRC Handbook of Chemistry and Physics," ed by D. R. Lide, CRC Press, New York (2002), pp. 6–116.
32 A. J. Tabor, "Gases, Liquids and Other States of Matter," 3rd ed, Cambridge University Press, Cambridge, U. K. (1991), Chapter 10.
33 M. H. March and M. P. Tosi, "Introduction to Liquid State Physics," World Scientific, New Jersey (2002), p. 269.